Structural and electronic property evolution of nickel and nickel silicide thin films on Si(100) from multicore x-ray-absorption fine-structure studies

S. J. Naftel, I. Coulthard, and T. K. Sham
Department of Chemistry, University of Western Ontario, London, Ontario, Canada, N6A 5B7

S. R. Das and D.-X. Xu
Institute for Microstructural Sciences, National Research Council, Ottawa, Ontario, Canada, K1A 0R6
(Received 24 July 1997)

We report an x-ray-absorption fine-structures (XAFS) investigation of a series of nickel and nickel silicide thin films prepared by magnetron sputtering nickel on Si(100) substrates and sequential annealing procedures. XAFS at the Ni *K* edge, Si *K* edge, and Si $L_{3,2}$ edge have been used to monitor the structure and bonding systematics at different stages of the silicidation process. It is found that the as-deposited film exhibits noticeable intermixing at the Ni-Si interface at room temperature, leading to the formation of a Ni-rich silicide in the vicinity of the interface; as the annealing temperature increases, predominantly NiSi and $NiSi_2$ phases are sequentially formed. It is also shown that Si $L_{3,2}$-edge studies using total electron yield and fluorescence yield are ideally suited for noninvasive characterization of silicide thin films. [S0163-1829(98)01115-1]

I. INTRODUCTION

Metal thin films on Si substrates and their interaction are of considerable interest in connection with the self-aligned silicidation (salicidation) process in which metal silicides are prepared by metal deposition on a Si(100) wafer followed by rapid thermal annealing (RTA). This technique is widely used in integrated circuits to reduce polysilicon interconnect resistance and silicon source/drain contact resistance in modern CMOS (complimentary metal oxide semiconductor) processes.[1,2] As device dimensions shrink, the electrical and mechanical integrity of the silicide with reduced vertical and lateral dimensions becomes an issue. It has been reported that titanium disilicide ($TiSi_2$), a commonly used silicide, exhibits significantly increased resistance as the lateral dimension shrinks to sub-half-micron.[3,4] It has also been reported that for nickel silicides,[3,5] the sheet resistance remains unchanged even for linewidths down to 0.1 μm, thus showing potential for applications in the next generation of ULSI (ultralarge scale integrated) circuits.

It appears that studies of the electronic structure systematics of metal-silicon interaction in unusual dimensions such as thin films, submicron lines, etc. will advance the understanding of the behavior of metal silicide films produced by the salicidation process. Information from these studies may in turn be used to modify the process. In this paper, we report a study using site and sampling depth sensitive core-level x-ray-absorption fine-structures (XAFS) to investigate a series of blanket nickel films on Si(100), representing stages before, during, and after silicidation.

II. EXPERIMENT

Ni films of a thickness of 50 nm were sputter deposited onto chemically clean, lightly P-doped, 4–7 Ω cm, *n*-type, Si(100) single-crystal substrates in a UHV magnetron sputtering system with a base pressure of $\leqslant 5\times10^{-7}$ Pa. Details of the chemical cleaning process and the sputter-deposition system have been described previously.[6] The deposition conditions for the specific films used in this investigation were Ar pressure, 2.00 Pa; Ar flow rate, 447 sccm; rf power 200 W; and target self-bias, −116 V. The Ni films were annealed *ex situ* at successively higher temperatures from 300 °C to 850 °C in steps of 50 °C for 30 sec at each temperature in dry N_2 ambient in an RTA (rapid thermal annealing) system. The specimens and their preparation conditions are summarized in Table I.

Si *K*-edge measurements were carried out at the Double Crystal Monochromator beamline of the Canadian Synchrotron Radiation Facility (CSRF) located at the Ednor M. Rowe Synchrotron Radiation Center, University of Wisconsin-Madison near Stoughton Wisconsin (800 MeV/1 GeV, typical injection current 250 mA). InSb(111) crystal monochromators were used. Si $L_{3,2}$-edge measurements were also carried out at the CSRF grasshopper beamline using a 1800 lines/mm grating, which provides a photon energy resolution of less than 0.1 eV at the Si $L_{3,2}$ edge (~100 eV). Ni *K*-edge measurements of the films were carried out with a Si(111) double crystal monochromator at the X11A beamline of the x-ray ring (2.5 GeV, typical injection current 200 mA) at the National Synchrotron Light Source (NSLS) at Brookhaven National Laboratory. Measurements at NSLS were carried out in a He atmosphere using both TEY (total

TABLE I. Summary of samples and preparation conditions.

Sample	Description
Ni-Si(1)	Ni (50 nm) on *n*-Si(100), as-deposited
Ni-Si(2)	Ni (50 nm) on *n*-Si(100), rapid thermal annealed at 300 °C/30 sec
Ni-Si(3)	Ni (50 nm) on *n*-Si(100), rapid thermal annealed at 300 °C/30 sec, 350 °C/30 sec, 400 °C/30 sec, 500 °C/30 sec
Ni-Si(4)	Ni (50 nm) on *n*-Si(100), rapid thermal annealed at 300 °C/ 30 sec, 350 °C/30 sec, 400 °C/30 sec, 850 °C/30 sec

electron yield) and FLY (fluorescence yield).[7] Measurements with soft x rays and VUV at CSRF were made in a vacuum chamber using both TEY (drained current) and FLY (channel plate detector).[8–12] The surface was degreased with organic solvents in an ultrasound bath prior to introduction into the chamber; ion sputtering was deliberately avoided.

Ni K-edge EXAFS (extended x-ray-absorption fine structures) were extracted from the absorption spectrum using standard procedures and were analyzed with Fourier transform (FT) techniques after background removal using a spline and normalization.[13] Bond lengths were obtained using the theoretical phase and amplitude package (FEFF6) of Rehr *et al.*[14]

III. MULTIELEMENT, MULTICORE XAFS

Let us consider for the moment the complexity of the system and how multielement, multicore XAFS can facilitate the understanding of the electronic structure of the system. When Ni is deposited on Si, intermixing may occur at the interface. Upon annealing, further intermixing and compound formation will take place. In order to probe the Ni silicide layers between the Si substrate underneath and the unreacted Ni overlayers, or native oxide on the surface when the film is exposed to the ambient, site and sampling depth selectivity is crucial. We show below that the multicore XAFS approach does provide some selectivity for the Ni-Si system.

We first consider the photoabsorption characteristics at Ni K(~8333 eV), Si K(~1840 eV), and $L_{3,2}$ (~100 eV) edges. The one absorption lengths ($1/e$ attenuation) are approximately 3.38 μm, 1.3 μm, and 50 nm for the Ni K edge, Si K edge, and Si $L_{3,2}$ edge, respectively, with corresponding core-hole lifetime broadenings of 1.44, 0.5, and 0.015 eV, respectively. It is apparent from the above information that the absorption coefficients alone immediately point to the near-surface and high chemical sensitivity of the Si $L_{3,2}$ edge because the one absorption length is comparable to typical film thickness (Table I) and the core-hole lifetime broadening is very narrow. Although the sampling depth sensitivity in yield measurements is also and more often than not determined by the escape depth of electrons and fluorescence photons,[15,16] in the case when the one absorption length is short, the photon penetrating depth becomes important as in the case of Si $L_{3,2}$ edge. Thin metal silicide films with the described thickness (Table I) will absorb practically all the incident photons at these energies.

The total electron yield technique is particularly sensitive to the first several nm of the film due to the short escape depth of the electrons in the solid;[8–12,15] therefore it is a preferred method for Ni and Si K-edge studies of thin nickel silicide films. Fluorescence technique samples at least ten times the depth[12,16] and is normally considered as a bulk technique for dilute samples and thin films. Thus a combined TEY and FLY study of the absorption spectrum of the films at the Si $L_{3,2}$ edge can reveal nondestructively both the surface (typically $\leqslant$1 nm) of the film that has been exposed to the ambient and the ''bulk'' metal-silicon layers ($>$50 nm) that are underneath with negligible influence from the Si substrate. Therefore, Si $L_{3,2}$-edge XAFS using FLY detection would reflect primarily the properties of the silicide film between the surface oxide and the Si substrate. In addition, since ion sputtering is not required for FLY, the risk of damage to the film by ion sputtering, which is required in photoemission experiments, is nonexistent.[17,18]

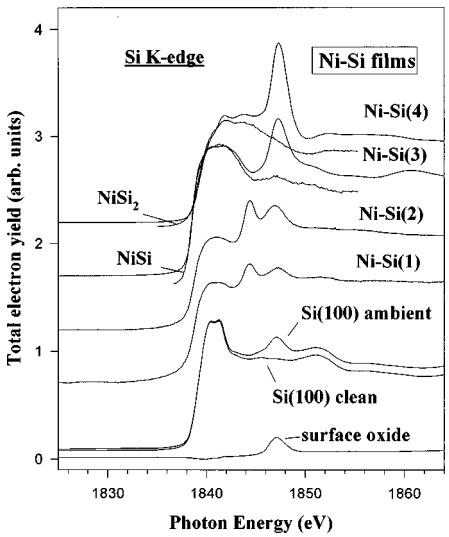

FIG. 1. Si K-edge XANES (TEY) for the Ni-Si system described in Table I.

It is clear from the above analysis that Si K edge with TEY detection is most sensitive to Si in the vicinity of the Ni-Si interface and in the Ni silicide layers, Ni K-edge (TEY) is most sensitive to the near surface Ni overlayers and Si $L_{3,2}$ edge with FLY detection is most sensitive to the ''bulk'' of the silicide film which is the main concern of this study.

IV. RESULTS AND DISCUSSION

General observations

Figure 1 shows the Si K-edge x-ray-absorption near-edge structure (XANES) obtained with TEY for the Ni-Si films (Table I) together with that of an ambient and a clean Si(100) wafer. The difference curve between ambient and clean Si(100), which represents the XANES of the surface native oxide (typically $<$1 nm)[12] is also shown. The corresponding FLY (not shown) exhibits only the XANES of crystalline Si. It is interesting to note that although the as-deposited film, Ni-Si(1) was covered with 50 nm Ni, we still see signals from the Ni-Si interface region and the substrate underneath. This is because the penetrating depth of the photon at the Si K edge is considerably larger than the thickness of the Ni film. The Si in the Ni-Si interface is most sensitive to Si K edge TEY detection since Ni absorption is monotonic in this energy region, it reduces the flux but does not modulate the Si K-edge XAFS. We can see from Fig. 1 that the as-deposited film, labeled Ni-Si(1), is noticeably different from that of clean Si(100) and significant changes occur upon further annealing.

Figure 2 shows the Ni K-edge XAFS of the exact films together with that of a Ni foil recorded in the TEY mode. FLY detection yields nearly identical XAFS for the films. In contrast to the Si K-edge results, the XAFS for the as-deposited film looks the same as that of the Ni foil while progressive change in both the XANES and EXAFS are evi-

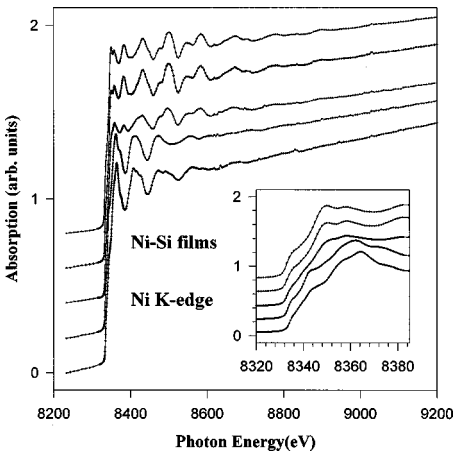

FIG. 2. Ni K-edge XAFS (TEY) for a Ni foil and the films; from top to bottom: Ni-Si(1); Ni-Si(2); Ni-Si(3); Ni-Si(4). The XANES are also shown in the same order in the inset.

dent upon annealing. These results readily suggest that Si and Ni K-edge XAFS recorded with TEY are probing different depths of the film.

The corresponding Si $L_{3,2}$-edge XANES for the films recorded by FLY are shown in Fig. 3 together with those recorded in TEY for a clean Si(100) wafer and the Ni-Si(3) film. Dramatic difference between TEY and FLY XANES for Ni-Si(3) and different spectral features for the films treated under different conditions are clearly visible.

Si and Ni K-edge XAFS

Let us first consider the most prominent features at the Si K edge for the as-deposited and the mildly annealed films shown in Fig. 1. The Si K-edge XANES of the as-deposited film, Ni-Si(1), and the film annealed to 300 °C, Ni-Si(2) (see Table I) exhibit XANES features significantly different from that of clean Si(100) at the Si K edge. Most noticeable are the presence of the resonances at ~1844 and 1847 eV and the broadening of the characteristic white line doublet for

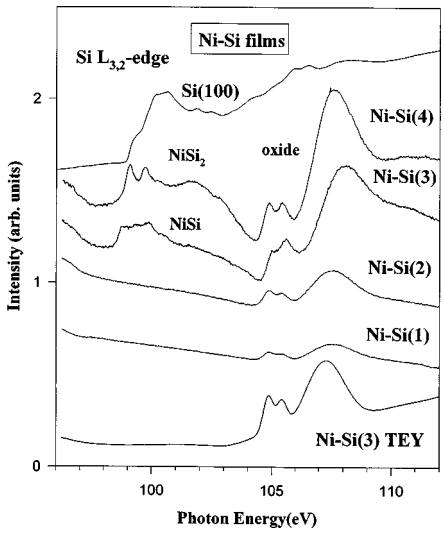

FIG. 3. Si $L_{3,2}$-edge XANES (FLY) for Ni-Si films, Ni-Si(1), Ni-Si(2), Ni-Si(3), and Ni-Si(4) ($NiSi_2$), the TEY for Ni-Si(3) is also shown.

crystalline silicon. A small shift (−0.4 eV) in threshold energy, defined as the point of inflection of the rising edge, is also seen. The widening of the white line and the blurring of the doublet indicate the presence of a new phase in which the long-range Si-Si interaction that results in the doublet is disrupted as a result of Ni-Si interaction.[19] This noticeable change must arise from intermixing between Si and Ni atoms at the interface and the interface Si signal contributes significantly to the Si K-edge spectrum. Since the film was prepared in a ultrahigh vacuum chamber and the Si surface was covered with 50 nm of Ni, the Si surface is well protected from oxidation; it is unlikely that these resonances are of an oxide origin unless the entire as-deposited film is converted to silicide; we show below that most of the Ni overlayer remains intact. Besides, silicon oxide, which exhibits a characteristic resonance at ~1847 eV, does not exhibit any significant feature below 1845 eV. The observation that the intensities for both resonances increase upon initial annealing with no change in spectral pattern and threshold energy indicates that further intermixing occurs without phase change [Ni-Si(2), Table I]. The intermixing would most likely yield a Ni-rich silicide phase with a characteristic resonance at 1844 eV. An estimate based on a recent depth profile analysis[12] shows that the region of intermixing at the interface is of the order of several nm.

As seen in Fig. 2, the Ni K edge of the as-deposited film Ni-Si(1) exhibits XAFS indistinguishable from that of a Ni foil in contrast to the Si K-edge results where the XANES for the as-deposited film is significantly different from that of Si(100). This result indicates that the Ni-Si intermixing evident in the Si K-edge spectra is confined to the vicinity of the interface of the as-deposited film and is not detected under the present experimental conditions. This is because Ni K-edge XAFS recorded by TEY is dominated by signals from the near surface region above the interface. For a 50-nm Ni film, for example, if the first ~40 nm Ni remains intact, the unreacted Ni will dominate the signal and the intermixed Ni-Si layers underneath would make relatively little contribution to the signal. The Ni K-edge XAFS for the film after modest temperature annealing [Ni-Si(2), 300 °C, Table I] shows a noticeable reduction (~40%) in amplitude and a broadening of the EXAFS oscillations although the pattern remains that of the fcc Ni. This together with the increase in Si K-edge resonance intensity at 1844 and 1847 eV for the Ni-rich silicide phase indicates that the thickness of the intermixing region has increased significantly and is moving towards the surface although it is still underneath the unreacted Ni overlayers. An estimate yields an upper bound of 30 nm. This situation is also confirmed by the corresponding Si $L_{3,2}$-edge TEY XANES (see below), which show no Si signal for these samples.

Annealing at higher temperature induces significant changes in the spectra. For Ni-Si(3) (500 °C, Table I), its Si K-edge XANES (Fig. 1) exhibits a much wider white line and the pattern characteristic of the Ni-rich phase and crystalline Si is no longer seen. A comparison of this spectrum with Si K-edge XANES for nickel silicides from the literature[20] shows that the film has been converted to NiSi. This is confirmed by x-ray diffraction. A θ-2θ scan in a diffractometer gave reflections at 2θ angles corresponding to reflections from different planes of the orthorhombic NiSi

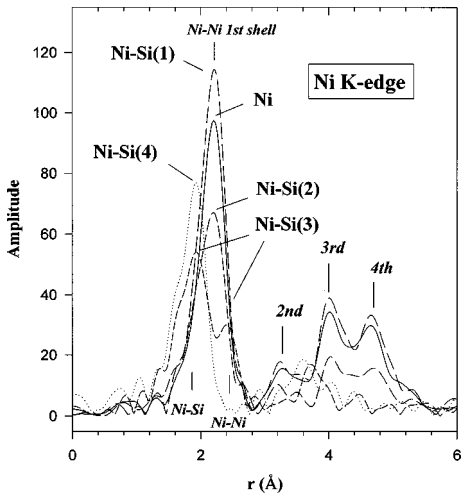

FIG. 4. Fourier transform of Ni K-edge EXAFS [$\chi(k)k^2$]. The vertical bars mark the positions of neighboring shells.

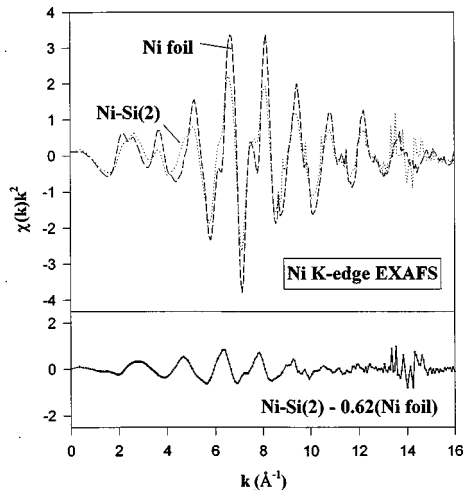

FIG. 5. Comparison of Ni K-edge EXAFS of Ni with Ni-Si(2). The difference curve after scaling the Ni EXAFS to match that of Ni-Si(2) is shown in the lower panel. This curve represents the Ni-Si EXAFS of Ni in the Ni-rich silicide in the vicinity of the interface.

phase. Auger electron spectroscopy further confirmed the composition as NiSi, which was uniform throughout the thickness of the layer. The corresponding Ni K-edge XAFS also changes drastically: the fcc-like oscillations are replaced by an entirely different pattern and new resonances emerge just above the threshold (inset, Fig. 2). The NiSi film exhibits shifts of -0.6 and 0.8 eV, respectively, at the Si and Ni K edge relative to the elements. Further annealing induces still another change as seen in the spectra for Ni-Si(4) (850 °C, Table I). The Si K edge (Fig. 1) shows some sharp features just above the threshold characteristic of localized densities of unoccupied states. The sharp resonance at 1847 eV is largely due to surface oxide and to a lesser extent the Si_2 dumbbell structure in all metal silicides with CaF_2 and $MoSi_2$ structures.[20–22] Surface oxides are inevitably present since the films have been exposed to the ambient after preparation.[23] A comparison with literature Si K-edge results[20] reveals that the film Ni-Si(4) is converted to a $NiSi_2$ phase. Again, this conclusion is confirmed by x-ray diffraction and Auger spectroscopy. This film exhibits no measurable edge shift in Si K edge but a noticeable shift of 1.5 eV at the Ni K edge. We show below that the nature of the film is also confirmed by the Ni K-edge EXAFS and that the threshold energy shift can be attributed to charge redistribution upon silicide formation.

Ni K-edge EXAFS

Figure 4 shows the Fourier transform of the EXAFS, $\chi(k)k^2$, for all the films as well as that of a Ni foil. It can be seen that the as-deposited film, Ni-Si(1), exhibits the usual pattern for fcc Ni of which the first several shells are clearly visible. The slight difference in amplitude between a thin Ni film on Si and a thick Ni foil is probably the result of thickness effect and perhaps a slightly different Debye-Waller factor for the film. These issues do not affect our discussion and will not be pursued further here. The most significant feature is the trend. The similarity between the FT of the as-deposited film and the Ni foil confirms that the intermixing of Ni and Si evident in the Si K-edge analysis is limited to the vicinity of the interface which contributes little to the Ni EXAFS. After the first annealing, the fcc pattern is still visible in Ni-Si(2) albeit with reduced amplitude and a shoulder at the smaller r side of the first-shell Ni-Ni peak emerges. The films, NiSi [Ni-Si(3)] and $NiSi_2$ [Ni-Si(4)], resulting from subsequent annealing at higher temperatures clearly show the expected radial distributions from their MnP and CaF_2 type crystal structures,[24] respectively. NiSi shows two peaks for the Ni-Si and Ni-Ni interatomic distances; the $NiSi_2$ result yields a Ni-Si interatomic distance of 2.328 ± 0.002 Å, in excellent agreement with results from previous analysis of $NiSi_2$ films[25] (2.37 ± 0.03 Å) and the bulk $NiSi_2$ value (2.336 Å). Using $NiSi_2$ as a reference we obtain the nearest Ni-Si and Ni-Ni interatomic distances of 2.34 ± 0.01 Å, and 2.69 ± 0.01 Å, respectively, for NiSi. We have also attempted to extract the average nearest Ni-Si interatomic distance in the interface by removing the Ni-Ni contribution to the overall XAFS signal in the K-edge data for Ni-Si(2). This was done by scaling and matching the Ni metal EXAFS to that of Ni-Si(2) so that their $\chi(k)k^2$ at $k > 12$ Å^{-1} coincide. This procedure is based on the fact that the Si backscattering amplitude peaks in the low-k region and decreases very rapidly in high k while the amplitude for Ni peaks in the mid-k region. This is illustrated in Fig. 5 where the difference curve is dominated by a single sinusoidal wave whose high-k region is nearly flat. Thus we can infer from the difference curve the average Ni-Si interatomic distance in the Ni-rich phase in the vicinity of the interface. FT analysis yields a value of 2.53 ± 0.01 Å which is longer than that of the Ni-Si bond in $NiSi_2$, but shorter than that in NiSi.

Si $L_{3,2}$-edge XANES

As noted above, the one absorption length at the Si $L_{3,2}$-edge photon energy (100 eV) and hence its fluorescence energy ($\sim$90 eV) as well, is $\sim$50 nm, directly comparable to the thickness of the film. Thus the FLY signal would be dominated by the bulk of the silicide film with negligible contributions from the Si substrate.

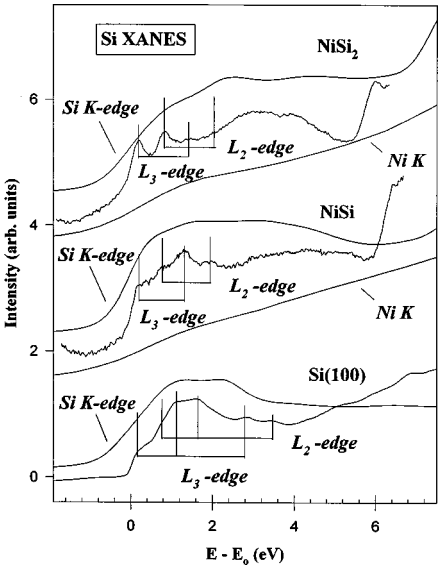

FIG. 6. Comparison of the Si K and $L_{3,2}$ edge XANES for NiSi, $NiSi_2$, and Si(100). Vertical bars mark the visible resonances for the Si L_3 and L_2 edges. The Ni K edge for the silicides are also shown.

Returning to Fig. 3, several important features are apparent. First, the dramatic change in sampling depths can be seen in the TEY and FLY XANES for the Ni-Si(3) film, which is essentially NiSi. The silicide spectrum, invisible in TEY, is clearly revealed in FLY. Second, there is a large chemical shift between the surface oxide and the silicides. This difference ($\sim$5 eV) together with high instrument resolution ($\sim$0.1 eV) provides a very useful chemical window to study the electronic structure of the silicide without the interference of the oxides which are inevitably present on the surface. Third, for the as-deposited and low-temperature annealed films, the interface cannot be revealed even by FLY since most of the incident and fluorescence photons are absorbed by the Ni films of which the upper layers remain intact. The result also indicates that no Si diffused to the surface. This confirms the Ni K-edge observation that the intermixing region is confined to the vicinity of the interface under the unreacted Ni overlayers. The oxide features for the silicide films are largely due to surface oxides and in the case of as-deposited and low-temperature annealed films due to scattered light detected by the channel plate which is made of silicon oxide. Both silicide and silicon oxide signals are absent in the TEY spectrum of Ni-Si(1) and Ni-Si(2) (not shown). Finally, from the figure we can clearly see a chemical shift of the Si L_3 and L_2 thresholds between the silicides and pure silicon; the shift is in the same direction as observed in the Si K edge: NiSi exhibits the largest shift (-0.5 eV) and $NiSi_2$ exhibits a smaller but measurable shift (-0.1 eV).

Charge redistribution upon silicidation

It is interesting to investigate the shifts in threshold energy (E_o) of the silicide films relative to the elements. The K edge arises from a transition of an electron from the $1s$ level to the lowest unoccupied state of p character (bottom of the conduction band in semiconductors and Fermi level in metals). It appears that the Si K edge E_o shifts to lower photon energy as Si becomes more dilute in Ni while the corresponding Ni K-edge threshold shifts to higher photon energy in the silicides. This result at its face value indicates that Si gains charge and Ni loses charge upon silicide formation. This is an interesting result in connection with electronegativity considerations since Pauling's scale shows that both Si and Ni have identical electronegativity. Thus the apparent charge transfer must be viewed in terms of charge redistribution. We argue that Ni favors $d \rightarrow s$ and Si favors $p \rightarrow s$ rehybridization upon silicide formation. This is reasonable since in the silicides, the Ni d-d interaction is reduced and the Si-metal bond will deviate significantly from sp^3 hybridization from the Si perspective. A reduction in $3d$ charge count at the Ni site will increase the binding energy of all the core levels even if the depletion is fully compensated by a gain of s charge, this is because the d charge is more compact and screens the nucleus better than the $4s$ charge. As for the Si, any change from sp^3 hybridization as well as metal Si bond formation will increase the s character at the Si site and hence the screening leading to negative shifts. It is conceivable that this parameter when measured accurately will contribute to the revelation of subtle changes in electronic structure of thin films and submicron lines.

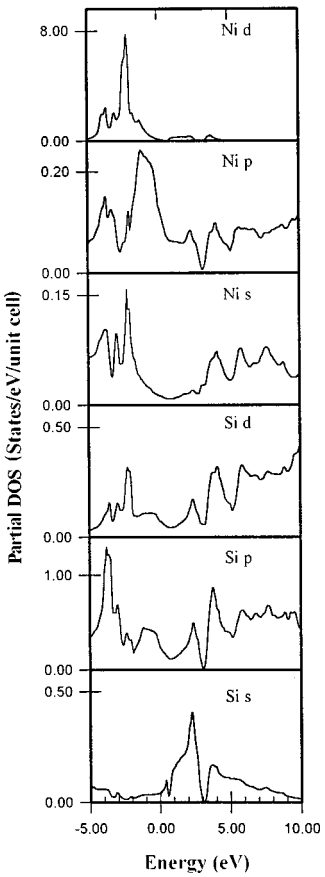

FIG. 7. Partial densities of states (PDOS) for Si and Ni in $NiSi_2$ from a recent calculation (Ref. 26). Fermi level is at 0 eV.

Correlation of XANES features with band calculations

Figure 6 shows the threshold region of the Si $L_{3,2}$ edge for the two films NiSi and $NiSi_2$, as well as Si(100) and their Si

and Ni K-edge counterparts aligned to the inflection point of the rising edge of the white line. Resonances for the Si L_3 and L_2 edges, separated by a spin-orbit coupling of 0.6 eV, are marked with vertical bars. The partial densities of states (PDOS) for $NiSi_2$ from a recent calculation[26] is also shown in Fig. 7. We have also carried out similar calculations, which yield almost exactly the same results. We see that the Si K and $L_{3,2}$ edge XANES for $NiSi_2$ is in qualitative agreement with the calculation in that the first two resonances at the Si $L_{3,2}$ edge correspond to the Si PDOS of s character within the first 3 eV above the Fermi level while the first three resonances at the Si K edge correspond to the three Si PDOS maxima of p character. The assignment for the $NiSi_2$ Ni K edge can also be made based on the calculation for the Ni PDOS although it is less certain due to weak absorption and core lifetime broadening: the first peak above the threshold corresponds to the first maximum of the Ni DOS of p and d character. No NiSi calculation is known to us but in the same work[26] the DOS for a Ni rich silicide, Ni_3Si was also calculated. The result shows two Si DOS maxima of p character within the first 5 eV above the Fermi level not inconsistent with our Si K-edge observation in the as-deposited and mildly annealed films (Fig. 1).

V. SUMMARY AND CONCLUSION

We have reported a series of x-ray-absorption experiments of nickel and nickel silicide thin films prepared on Si(100) by magnetron sputtering nickel and subsequent annealing processes. We show that by using different core levels, we can enhance the XAFS probing capability by sampling different atomic sites and depths from the surface. The use of Ni K, Si K, and Si $L_{3,2}$ edge XAFS in this study allows us to monitor the electronic interaction at various stages of the silicidation process. Of particular interest is the Si $L_{3,2}$ edge using TEY and FLY detection schemes where the inherent narrow core levels and chemical shifts between silicon oxide and silicide, and the suitable sampling depth provides an excellent opportunity to monitor the systematics of the electronic structure of these films in some detail. The results reported here clearly show that single phase NiSi and $NiSi_2$ blanket films can be prepared under controlled conditions. Noticeable threshold energy shift between silicide and pure element is observed despite identical electronegativity for Ni and Si, and is attributed to charge redistribution. The XANES features are in good agreement with DOS calculations indicating that the XANES features are of a single particle origin and can be used to identify the phase of the silicide films. These techniques are now being extended to the study of submicron metal silicide lines.

ACKNOWLEDGMENTS

The research at UWO was supported by NSERC of Canada. The Ednor M. Rowe Synchrotron Radiation Centre, University of Wisconsin-Madison, and NSLS at Brookhaven National Laboratory are supported by the U.S. National Science Foundation under Award No. DMR-95-31009 and the U.S. Department of Energy under Contract No. DE-AC02-76CH00016, respectively.

[1] See, for example, Appl. Surf. Sci. **53**, (1991); the entire volume deals with metal silicide and its application in microelectronics.

[2] See, for example, S. P. Murarka, *Metallization-Theory and Practice for VLSI and ULSI* (Butterworth-Heinemann, Boston, MA, 1993).

[3] T. Ohguro, S. Nakamura, M. Koike, T. Morimoto, A. Nishiyama, Y. Ushiku, T. Yoshitomi, M. Ono, M. Sato, and H. Iwai, IEEE Trans. Electron Devices **41**, 2305 (1994).

[4] C. Blair, E. Demirlioglu, E. Yoon, and J. Pierce, in *Silicides, Germanides, and Their Interfaces*, edited by R. W. Fathauer, L. Schowalter, S. Mantl, and K. N. Tu, MRS Symp. Proc. No. 320 (Materials Research Society, Pittsburgh, 1994), p. 53.

[5] D.-X. Xu, S. R. Das, L. Erickson, and A. Naem, in *Materials Reliability in Microelectronics V*, edited by A. S. Oates, K. Gadepally, R. Rosenberg, W. F. Filter, and L. Greer, MRS Symp. Proc. No. 391 (Materials Research Society, Pittsburgh, 1995), p. 233.

[6] S. R. Das. D.-X. Xu, J. Phillips, J. McCaffrey, L. LeBrum and A. Naem, in *Interface Control of Electrical, Chemical, and Mechanical Properties*, edited by S. P. Murarka, K. Rose, T. Ohmi, and T. Seidel, MRS Symp. Proc. No. 318 (Materials Research Society, Pittsburgh, 1994), p. 129.

[7] W. T. Elam, J. P. Kirkland, R. A. Neiser, and P. D. Wolf, Physica B **158**, 295 (1989).

[8] A. Erbil, G. S. Cargill, III, R. Frahm, and R. F. Boehme, Phys. Rev. B **37**, 2450 (1988).

[9] J. Stohr, *NEXAFS Spectroscopy*, Springer Series in Surface Science Vol. 25 (Springer, Berlin, 1992).

[10] F. Comin, L. Incoccia, P. Lagarde, G. Rossi, and P. Citrin, Phys. Rev. Lett. **54**, 122 (1985).

[11] M. Kasrai, Z. Yin, G. M. Bancroft, and K. H. Tan, J. Vac. Sci. Technol. A **11**, 2694 (1993).

[12] M. Kasrai, W. N. Lennard, R. W. Brunnder, G. M. Bancroft, J. A. Bardwell, and K. H. Tan, Appl. Surf. Phys. **99**, 303 (1996).

[13] The analysis is done with a software package provided by T. Tylisczcik of McMaster University. The FEEF data base from J. J. Rehr of the University of Washington was used.

[14] J. J. Rehr, J. Mustre deLeon, S. I. Zabinsky, and R. C. Albers, J. Am. Chem. Soc. **113**, 5135 (1991).

[15] The sampling depth for TEY has been discussed extensively in Refs. 7–10; also see J. Stohr, C. Noguera, and T. Kendelewicz, Phys. Rev. B **30**, 5571 (1984); and T. K. Sham and R. Carr, J. Chem. Phys. **83**, 5914 (1985).

[16] A. Hiraya, M. Watanabe, and T. K. Sham, Rev. Sci. Instrum. **66**, 1528 (1995).

[17] S. J. Naftel, T. K. Sham, S. R. Das, and D.-X. Xu, in *Thin Films-Structure and Monophology*, edited by S. C. Moss, D. Ila, R. C. Cammarata, E. H. Chason, T. L. Einstein, and E. A. Williams, MRS Symp. Proc. No. 441 (Materials Research Society, Pittsburgh, 1997), p. 175.

[18] G. Rossi, Surf. Sci. Rep. **7**, 1 (1987).

[19] T. K. Sham, X.-H. Feng, D. T. Jiang, B. X. Yang, J. Z. Xiong, A. Bzowski, D. C. Houghton, B. Bryskiewicz, and Wang, Can. J. Phys. **70**, 813 (1992).

[20] (a) P. J. W. Weij, M. T. Czyzyk, J. F. van Acker, W. Speier, J. B. Goedkoop, H. van Leuken, H. J. M. Hendrix, R. A. de Groot, G. van der Laan, K. H. Buschow, W. Weich, and J. C. Fuggle, Phys. Rev. B **41**, 11 899 (1990); (b) P. Lerch, T. Jarlborg, V. Codazzi, G. Loupias, and A. M. Flank, Phys. Rev. B **45**, 11 481 (1992).

[21] W. F. Pong, Y. K. Chang, R. A. Mayanovic, S. H. Ko, P. K. Tseng, C. T. Cheng, A. Hiraya, and M. Watanabe, Phys. Rev. B **53**, 16 510 (1996).

[22] S. J. Naftel, T. K. Sham, V. Smelyanski, J. S. Tse, and J. D. Garrett, J. Phys. IV **7**, C2-495 (1997).

[23] In another series of experiments, we studied a series of MSi_2 compounds and confirmed the presence of a resonance at ~1847 eV for silicides with a Si_2 dumbbell unit such as in $CoSi_2$ and $MoSi_2$.

[24] Crystal structures for $NiSi_2$ and NiSi can be found in *Atlas of Crystal Structure Type for Intermetallic Phases,* edited by L. J. C. Daams, P. Villars, and J. H. N. van Vucht (ASM International, Metals Park, OH, 1991).

[25] F. Comin, J. E. Rowe, and P. H. Citrin, Phys. Rev. Lett. **51**, 2402 (1983).

[26] A. Gheorghiu, C. Senemaud, E. Belin-Ferre, Z. Dankhazi, L. Magaud-Martinage, and D. A. Papaconstantopoulos, J. Phys.: Condens. Matter **8**, 719 (1996).